Nonlinear and chaotic oscillations of an india-rubber band

R. Chacón, P. Suárez, and F. Sánchez-Bajo
Departamento de Electrónica e Ingeniería Electromecánica, Escuela de Ingenierías Industriales, Universidad de Extremadura, Apartado Postal 382, 06071 Badajoz, Spain

P. Muñiz
Departamento de Física Aplicada, Universidad de Castilla–La Mancha, Campus Universitario, 13071 Ciudad Real, Spain
(Received 30 September 1996; revised manuscript received 8 July 1997)

The restoring force of a length of stretched elastic band is studied experimentally and the comparison with that of a spring is discussed. It is demonstrated that the simplest model of elastic band oscillations is capable of showing nonlinear phenomena including crisis, periodic, and chaotic motions, as well as spatial symmetry breaking. [S1063-651X(97)09211-8]

PACS number(s): 05.45.+b, 05.40.+j

I. INTRODUCTION

A great deal of attention has been paid in the past few decades to the study of nonlinear oscillations of elastic springs [1–9], although the earliest studies go back to the past century [10]. In addition to their scientific interest, springs appear in almost all physics textbooks, at secondary and university levels [11,12], as the simplest model for both linear and nonlinear oscillations. However, a length of ordinary (cut) elastic india-rubber band (henceforth termed ''elastic band'') is another of the simplest spatially distributed nonlinear systems imaginable: In addition to its intrinsic theoretical interest, the nonlinear dynamics of an elastic band could also shed light on the dynamics of more complicated systems with spatial distribution (e.g., hydrodynamic systems). The main purpose of this work is to reveal the characteristics of the restoring force of a common elastic band.

The paper is organized as follows. In Sec. II we propose an analytical expression for the restoring force of a stretched elastic band that is in excellent agreement with our experimental results. A comparison is also made with the restoring force corresponding to a stretched nonlinear elastic spring. In Sec. III we study a very simple single-mode model of elastic-band oscillations deduced from the phenomenological restoring force postulated in Sec. II and demonstrate that the vibrating elastic band can undergo spatial symmetry breaking and crisis as well as periodic and chaotic motions. We concentrate on the structural stability of the model system under changes in an elastic-band characteristic parameter. Finally, Sec. IV gives a summary of the results.

II. EXPERIMENTAL ELASTIC-BAND RESTORING FORCE

We studied experimentally the elastic response of lengths of (common) stationer's elastic bands subjected to stretching. The samples were in the form of ribbons with different dimensions. The experiments were carried out in a mechanical testing machine controlled by computer, in all cases at the same temperature ($\sim 25\,^{\circ}$C). The specimens were gripped between a stationary lower and a movable top clamp. The movable part contained a force controller that measured up to 100 N. The experiments were carried out in two ways: (a) controlling the displacement of the movable part with a constant stretching rate (50 mm/min) and (b) controlling the added load rate (0.1 N/min or 0.5 N/m). In both cases the computer records the load and longitudinal stretch every 0.05 s. We found very similar results for the two types of experiments: A typical example is plotted in Fig. 1 (thick line). Observe the initial smooth hump, forming a first nonlinear region of elasticity, which is the characteristic feature of the elastic band distinguishing it from, for example, an elastic spring [13]. A second broader region of nonlinearity (after the inflection point) is common to elastic springs [13].

To take these characteristics into account we propose the following analytical expression for the restoring force:

$$F(x) = -k\left[x\left(2-\tanh\left|\frac{x}{a}\right|\right)+bx^3\right], \tag{1}$$

where x is the displacement from the relaxed position, k is a strength parameter, a is an *elastic-band characteristic pa-*

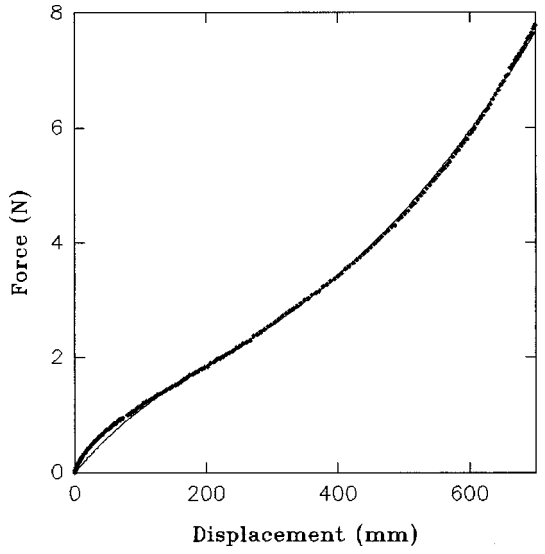

FIG. 1. Experimental restoring force (thick line) of a stretched elastic band and theoretical fit (thin line) [Eq. (1)] for $k = 0.0068$ N/mm, $a = 236$ mm, and $b = 1.23\times10^{-6}$ mm.

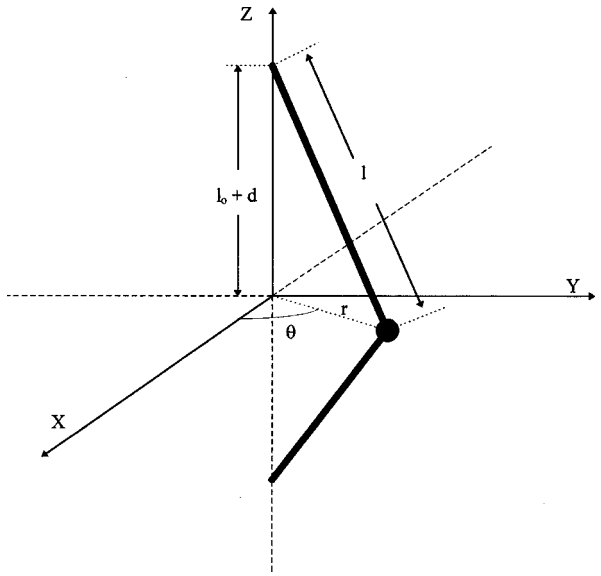

FIG. 2. Single-mode model for nonlinear oscillations of an elastic band. The oscillations are assumed to be in the fundamental mode and are measured in the transverse x-y plane in terms of polar coordinates (r,θ).

rameter that controls the shape of the aforementioned smooth hump [$F(x)\approx kx$ for the second linearity region, $x \approx 3a$], and b is the (main) nonlinearity parameter that is responsible for the wider and stronger nonlinearity region. The best nonlinear least-squares Levenberg-Marquardt fit to the experimental example plotted in Fig. 1 was with $k = 0.0068$ N/mm, $a = 236$ mm, and $b = 1.23\times 10^{-6}$ mm^{-2} (thin line). Similarly good fits were found to the other experimental results by suitably choosing the parameters k,a,b for each case.

It is illuminating to consider the limiting cases $a\to 0,\infty$ for the restoring force (1). Indeed, we obtain

$$\lim_{a\to\infty} F(x) = -k(2x + bx^3), \tag{2}$$

$$\lim_{a\to 0} F(x) = -k(x + bx^3), \tag{3}$$

i.e., the two limits correspond to nonlinear springs with Hooke's elastic constants $2k$ and k, respectively.

III. DYNAMICS OF AN ELASTIC-BAND MECHANICAL MODEL

The simplest model of an elastic band oscillating in its fundamental mode is illustrated in Fig. 2. The ends of a massless elastic band are fixed a distance $2(l_0+d)$ apart, where the relaxed length of the elastic band is $2l_0$ and its parameters are k,a,b [cf. Eq. (1)]. Note that at the equilibrium position the elastic band is stretched a length $2d$ (we assume that the ends of the elastic band are fixed symmetrically). To the center of the elastic band is attached a particle of mass m that is free to oscillate in the x-y plane around the origin. According to Eq. (1), the restoring force on the particle is

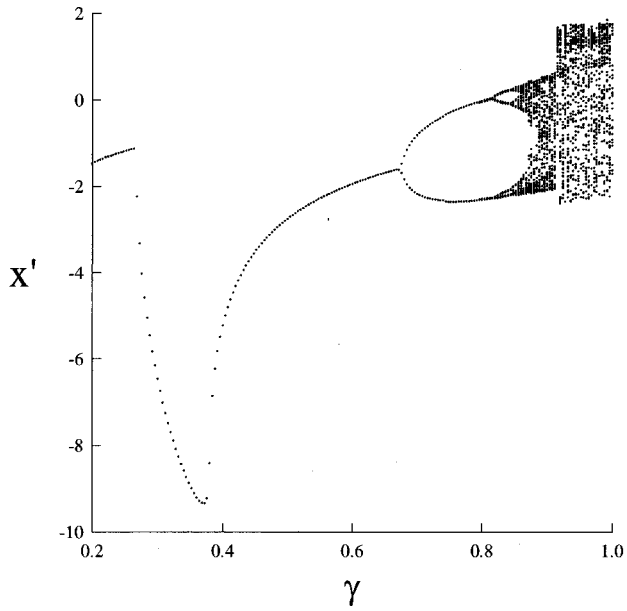

FIG. 3. Global bifurcation diagram for the variable x', with $A = 28.5$, $\delta = 0.2$, $\omega = 0.86$, and γ in the range $0.2 \leqslant \gamma \leqslant 1$.

$$F = -\frac{2kr}{l}\left\{(l-l_0)\left[2-\tanh\left|\frac{l-l_0}{a}\right|\right]+b(l-l_0)^3\right\}, \tag{4}$$

where the position of the particle is given in terms of polar coordinates (r,θ) of the x-y plane. Expanding the right-hand side of Eq. (4) in a series ($r \ll l_0$, $d \ll l_0$), we obtain

$$F = -4\left(\frac{kd}{l_0}\right)r - \frac{2k}{l_0^2}\left[1-\frac{d}{a}-3\,\frac{d}{l_0}\right]r^3 + O\left(\frac{d^2}{l_0^2},\,\frac{r^3}{l_0^3}\right), \tag{5}$$

i.e., we can approximate the equation of motion by

$$\ddot{\mathbf{r}} + \omega_0^2\mathbf{r}(1+\alpha_{eb}\mathbf{r}^2) = 0, \tag{6}$$

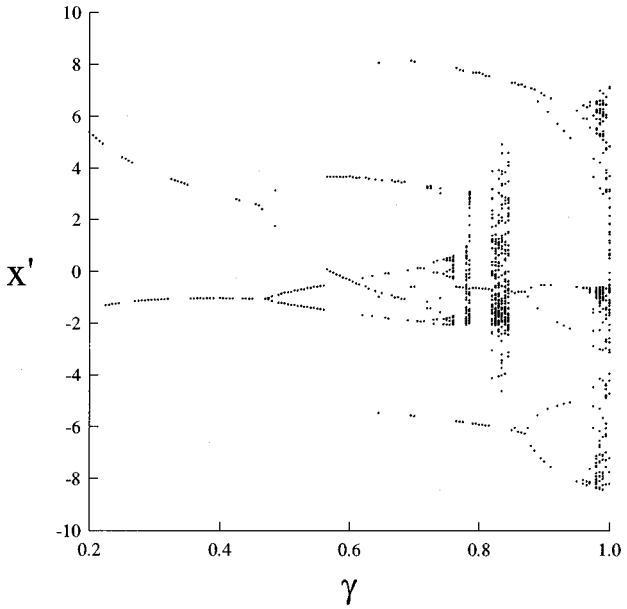

FIG. 4. Global bifurcation diagram for the variable x', with $A = 27$, $\delta = 0.2$, $\omega = 1.34$, and γ in the range $0.2 \leqslant \gamma \leqslant 1$.

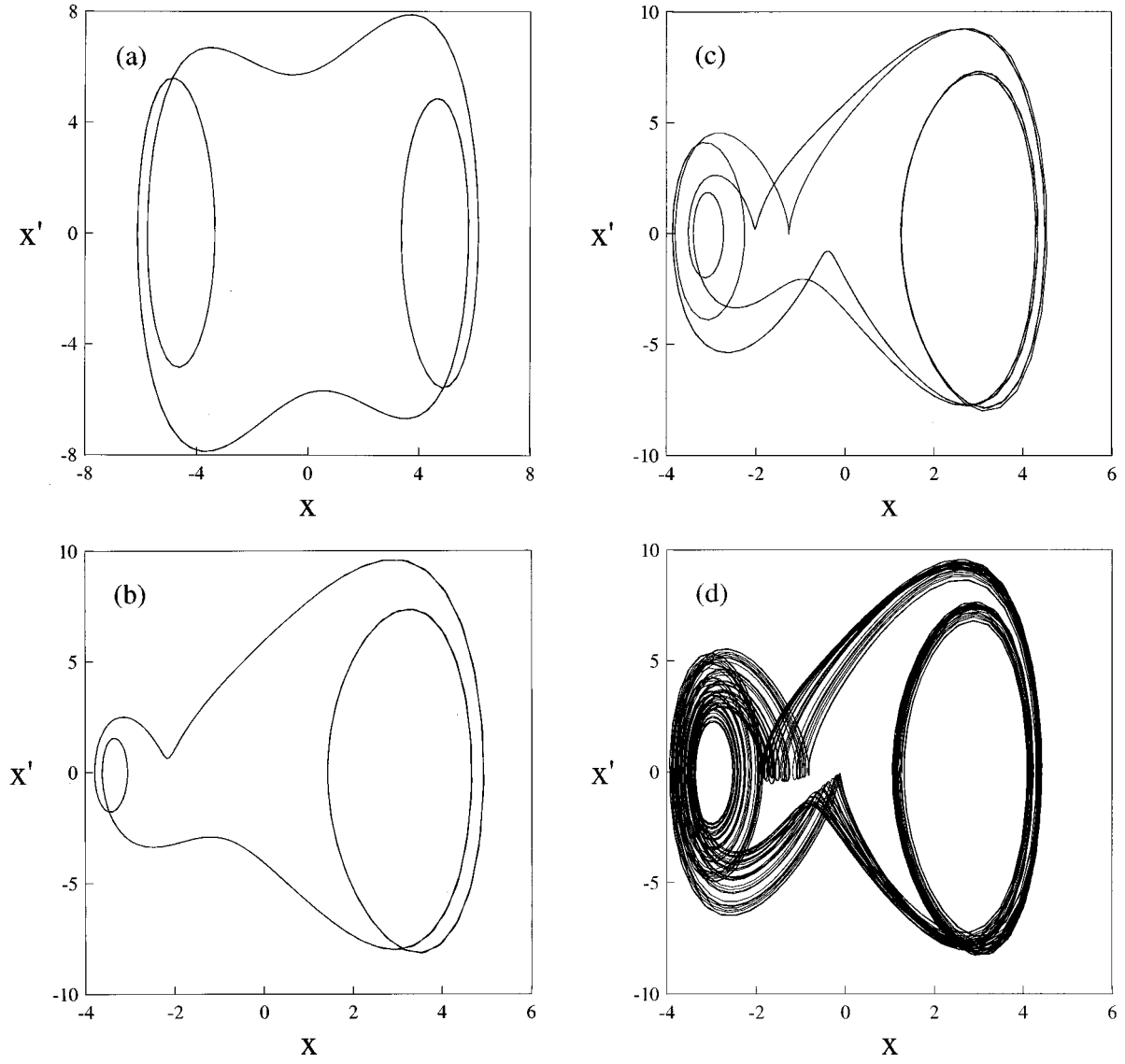

FIG. 5. Phase-space portraits for the parameter $\delta=0.2$, $A=28.5$, and $\Omega=0.86$. (a) Symmetric orbit ($\gamma=0.2$), (b) followed by symmetry breaking ($\gamma=0.6$), (c) by period doubling ($\gamma=0.8$), and then (d) by chaos ($\gamma=0.91$).

where

$$\omega_0^2 \equiv 4kd/ml_0,$$

$$\alpha_{eb} \equiv [a(l_0-3d)-dl_0]/2dal_0^2, \tag{7}$$

which corresponds to a two-dimensional conservative cubic oscillator with a single potential well $[a>l_0 d/(l_0-3d)]$. Observe that the nonlinearity parameter α_{eb} increases with increasing elastic-band characteristic parameter a. This is the main difference with respect to the corresponding spring problem at the same perturbative order (cf. Refs. [9, 13]). Indeed, for the spring counterpart, under a similar approximation, one finds [13]

$$F \approx -\frac{2k'd}{l_0}\, r - \frac{k'}{l_0^2}\left(1-3\frac{d}{l_0}\right) r^3, \tag{8}$$

with k' being the spring parameter ($k' \equiv 2k$; cf. Sec. II). However, in the limit $d \to 0$, both systems are described by the same intrinsically nonlinear cubic oscillator. The respective equation of motion for Eq. (8) is given by

$$\ddot{\mathbf{r}} + \omega_0^2 \mathbf{r}(1+\alpha_s \mathbf{r}^2) = 0, \tag{9}$$

where

$$\alpha_s \equiv (l_0-3d)/2dl_0^2. \tag{10}$$

A comparison between α_{eb} [cf. Eq. (7)] and α_s gives

$$\alpha_s - \alpha_{eb} = 1/2al_0, \tag{11}$$

with $\alpha_{eb} \to \alpha_s$ as $a \to \infty$, in agreement with the discussion in Sec. II.

In general, we will want to consider forcing and damping, so Eq. (6) is rewritten

$$\ddot{\mathbf{r}} + \omega_0^2 \mathbf{r}(1+\alpha_{eb}\mathbf{r}^2) + \beta\dot{\mathbf{r}} = \mathbf{P}(t), \tag{12}$$

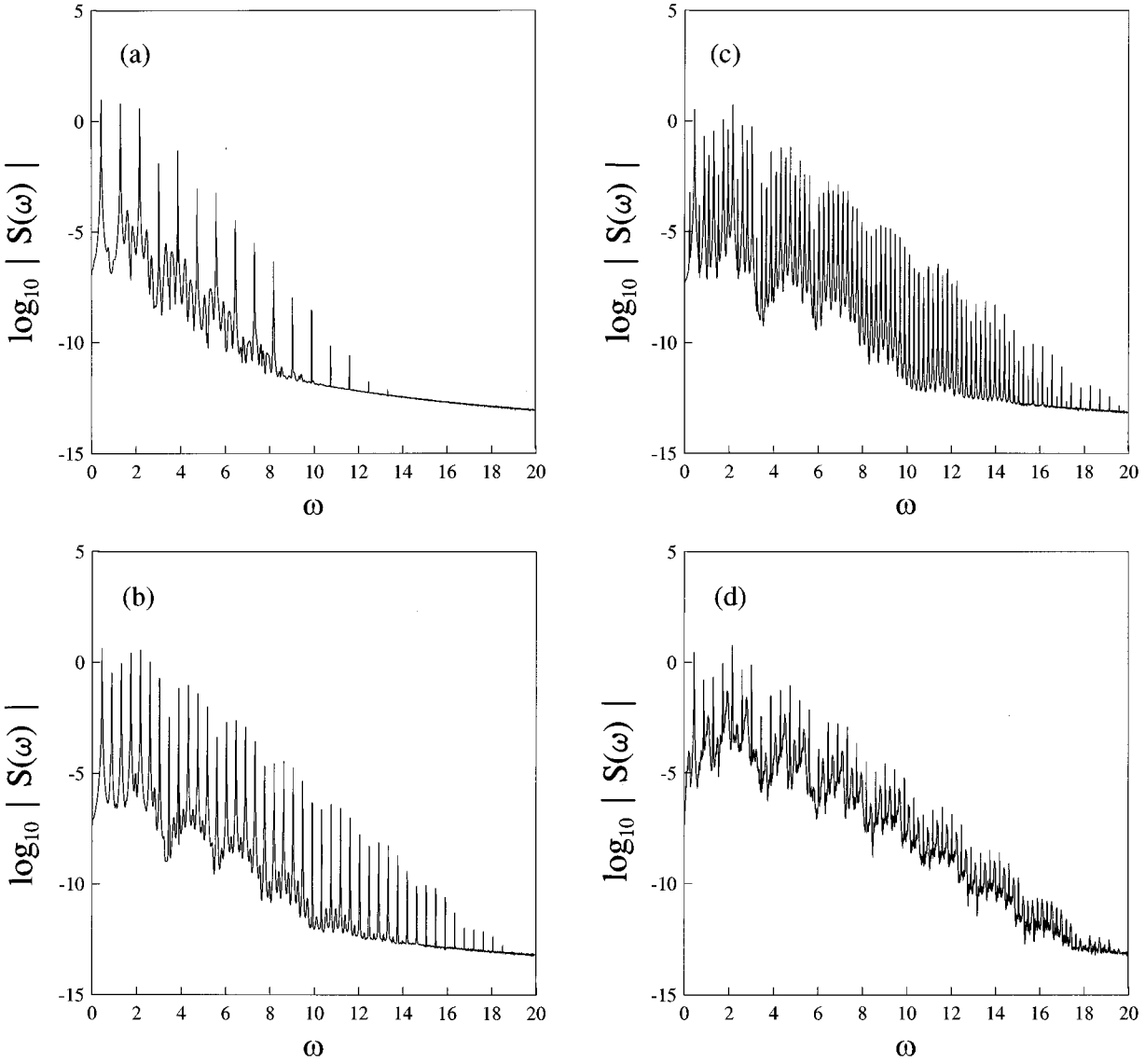

FIG. 6. Power spectra corresponding to the respective cases in Fig. 5 showing the following sequence: (a) symmetric orbit (odd subharmonics), (b) symmetry breaking (odd plus even subharmonics), (c) period doubling, and (d) chaos.

where $\mathbf{P}(t)$ is a T-periodic forcing term and β is the damping coefficient (which is a scalar due to the symmetry of the system). In order to facilitate the comparison between theoretical and (future) experimental results, Eq. (12) can be rewritten in dimensionless form. To this end, consider the transformation

$$\tau=\omega_0 t, \quad \mathbf{q}=\mathbf{r}/l_0, \tag{13}$$

giving

$$\mathbf{q}''+\mathbf{q}(1+\gamma\mathbf{q}^2)+\delta\mathbf{q}'=\mathbf{G}(\tau/\omega_0), \tag{14}$$

where the prime denotes differentiation with respect to τ and

$$\gamma\equiv\alpha_{eb}l_0^2, \quad \delta\equiv\beta/\omega_0, \quad \mathbf{G}\equiv\mathbf{P}/l_0\omega_0^2. \tag{15}$$

For the sake of simplicity, suppose that the ends of the elastic band are fixed in such a way that the oscillation is confined to a single plane. The nonlinear equation of motion for an elastic band vibrating primarily in its fundamental mode is a forced Duffing equation [14] of the form

$$x''+x(1+\gamma x^2)=-\delta x'+G(\tau/\omega_0), \tag{16}$$

where Eq. (16) is obtained from Eq. (14) by assuming that the dynamics is confined to the x-z plane (see Fig. 2). In this paper we will take the forcing term to have the form of a harmonic modulation

$$G(\tau/\omega_0)=A\cos(\Omega\tau), \tag{17}$$

with $\Omega\equiv 2\pi/T\omega_0$.

The simplest way to visualize the differences between spring and elastic-band vibrations is to study the evolution of the attracting orbits as only the elastic-band characteristic parameter a [and hence γ; cf. Eqs. (7) and (15)] is varied. To this end we will construct global bifurcation diagrams (x' vs γ) and phase-space diagrams (x' vs x) for planar motion modeled by the Duffing oscillator forced only in the x direc-

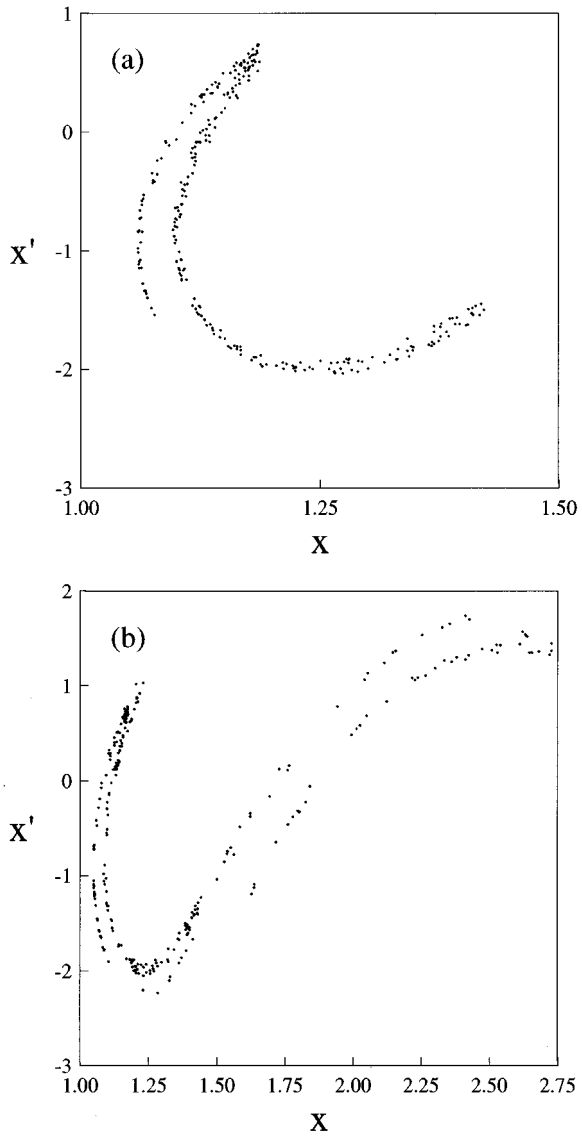

FIG. 7. Bidimensional Poincaré sections illustrating the crisis process for the same parameters as in Fig. 3. (a) $\gamma=0.91$, chaotic attractor associated with the period-doubling cascade, and (b) $\gamma=0.92$, the jump in size of the chaotic attractor should be noted.

tion by a harmonic term [Eqs. (16) and (17), respectively]. To integrate the differential equations we used a fourth-order Runge-Kutta method with time steps in the range $\Delta\tau=0.005-0.01$. In most of the numerical simulations $\delta=0.2$, $A=\{28.5,27\}$, $\Omega=\{0.86,1.34\}$, and the nonlinearity parameter γ ranged from 0.2 to 1. Another way of characterizing the phenomenon is by looking at the spectral properties of the solutions. The numerical integration yields pseudo-orbits of the system in the form of time series $x(t),x'(t)$; a standard fast Fourier transform then yields the power spectrum $S(\omega)=|a(\omega)|^2$. Usual averaging procedures were used to improve its quality [15].

In order to appreciate to some extent the global dynamical behavior of the model system (16) and (17) as the parameter γ is varied, we have determined global bifurcation diagrams corresponding to the variable x' for two different sets of parameters (Figs. 3 and 4). Figure 5 shows the evolution of the phase-space portraits for increasing nonlinearity param-

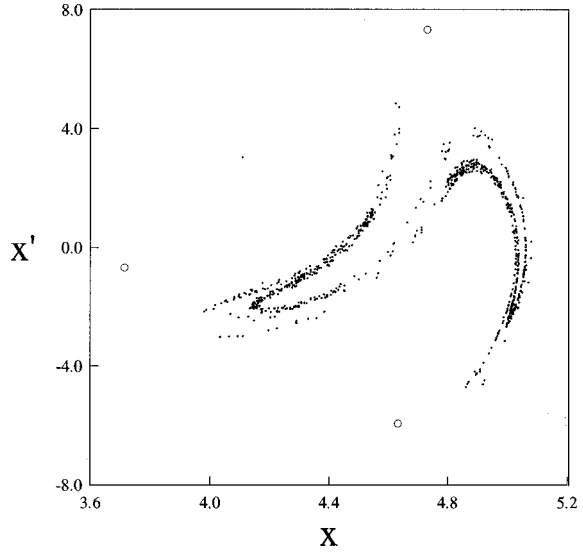

FIG. 8. Bidimensional Poincaré section simultaneously showing the period-3 attractor (circles) for $\gamma=0.81$ and the chaotic attractor for $\gamma=0.82$. The remaining parameters are the same as in Fig. 4.

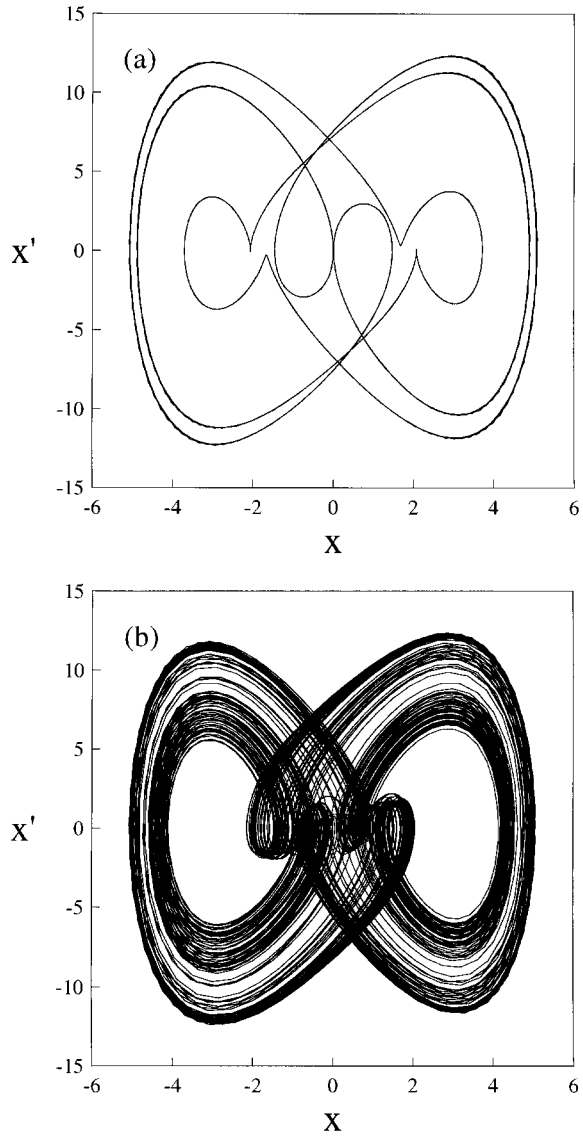

FIG. 9. Phase-space steady-state trajectories corresponding to the attractors in Fig. 8. (a) $\gamma=0.81$ and (b) $\gamma=0.82$.

eter γ and the remaining parameters fixed at the same values as in Fig. 3. The associated power spectra, corresponding to the $x'(t)$ series, are plotted in Fig. 6. For small values of γ the orbit is symmetric [see Figs. 3 and 5(a)] with peaks corresponding only to odd subharmonics in the associated power spectrum [Fig. 6(a)]. However, for $\gamma \geqslant 0.3$ the orbits become spatially asymmetric [Figs. 3 and 5(b)], which is reflected in the visible presence of even subharmonics in the corresponding power spectrum [Fig. 6(b)]. This *symmetry breaking* of the Duffing oscillator appears to be a precursor of the period-doubling route for chaos [Figs. 3, 5(c), and 6(c)]. This type of phenomenon was found by D'Humieres *et al.* [16] in a driven pendulum with increasing forcing amplitudes [17]. For larger values of γ the system undergoes an interior crisis in the sense of Grebogi, Ott, and Yorke [17]. The period-doubling chaotic attractor resulting at $\gamma = 0.91$ [Fig. 7(a)] suddenly blows up to a large chaotic attractor $\gamma = 0.92$ [Fig. 7(b)]. As a final example, Fig. 8 shows the Poincaré sections corresponding to period-3 and chaotic attractors for $\gamma = 0.81$ and 0.82, respectively, the remaining parameters fixed at the same values as in Fig. 4. The associated steady-state trajectories are plotted in Figs. 9(a) and 9(b), respectively.

IV. CONCLUSION

We have studied experimentally the restoring force arising from an elastic band, comparing it with that from an elastic spring. It was shown that the simplest model for damped and forced oscillations of the band is capable of exhibiting several nonlinear phenomena, including crisis as well as spatial symmetry breaking as a precursor to the period-doubling route for chaos. We believe that the comparison between theory and experiment for this model could provide valuable information about the nonlinear dynamics of spatially extended systems. Of course, with the onset of chaotic motion it is reasonable to expect that this single mode will lose applicability since chaotic behavior implies the excitation of several modes, so that the formulation of a multimode model would seem appropriate. In sum, the general problem of the ''excitation of multiple modes'' by chaotic oscillations might be fruitfully investigated by combining experimental and theoretical studies of vibrating elastic bands.

[1] N. Minorsky, *Nonlinear Oscillations* (Krieger, Malabar, FL, 1962), pp. 51–53.
[2] K. S. Mendelson, J. Math. Phys. **11**, 3413 (1970).
[3] H. R. Baum, Q. Appl. Math. **30**, 573 (1972).
[4] R. Broucke and P. A. Baxa, Celest. Mech. **8**, 261 (1973).
[5] M. Kuroda, Bull. JSME **17**, 59 (1974).
[6] T. Jamamoto, Y. Ishida, and J. Kawasumi, Bull. JSME **18**, 965 (1975).
[7] J. Kevorkian and J. D. Cole, *Perturbation Methods in Applied Mathematics* (Springer-Verlag, New York, 1981), pp. 17–28.
[8] H. N. Núñez-Yepes, A. L. Salas-Brito, C. A. Vargas, and L. Vicente, Phys. Lett. A **145**, 101 (1990).
[9] J. Awrejcewicz, *Bifurcation and Chaos in Coupled Oscillators* (World Scientific, Singapore, 1991), pp. 120–148.
[10] Lord Rayleigh, *The Theory of Sound* (Macmillan, London, 1894).
[11] P. A. Tipler, *Physics for Scientists and Engineers* (Worth, New York, 1991), Vol. 1, pp. 368–408.
[12] R. P. Feynman, R. B. Leighton, and M. Sands, *The Feynman Lectures on Physics* (Addison-Wesley, Reading, MA, 1963), Vol. 1, Chap. 21.
[13] J. B. Marion, *Classical Dynamics of Particles and Systems* (Academic, New York, 1970), pp. 172–175.
[14] See, e.g., J. Guckenheimer and P. Holmes, *Nonlinear Oscillations, Dynamical Systems and Bifurcation of Vector Fields* (Springer-Verlag, New York, 1983), pp. 82–91.
[15] W. H. Press, B. P. Flannery, S. A. Teukolsky, and W. T. Vetterling, *Numerical Recipes. The Art of Scientific Computing* (Cambridge University Press, Cambridge, 1988), pp. 381–453.
[16] D. D'Humieres, M. R. Beasly, B. A. Huberman, and A. Libchaber, Phys. Rev. A **26**, 3483 (1982).
[17] C. Grebogi, E. Ott, and J. A. Yorke, Phys. Rev. Lett. **48**, 1507 (1982); Physica D **7**, 181 (1983).